Segmentation of Cortical MS Lesions on MRI Using Automated Laminar Profile Shape Analysis

Christine L. Tardif[1], D. Louis Collins[1], Simon F. Eskildsen[2], John B. Richardson[3], and G. Bruce Pike[1]

[1] McConnell Brain Imaging Centre, Montreal Neurological Institute, Canada
[2] Dept. of Health Science and Technology, Aalborg University, Denmark
[3] Dept. of Neuropathology, Montreal Neurological Institute/Hospital, Canada

Abstract. Cortical multiple sclerosis lesions are difficult to detect in magnetic resonance images due to poor contrast with surrounding grey matter, spatial variation in healthy grey matter and partial volume effects. We propose using an observer-independent laminar profile-based parcellation method to detect cortical lesions. Following cortical surface extraction, profiles are extended from the white matter surface to the grey matter surface. The cortex is parcellated according to profile intensity and shape features using a k-means classifier. The method is applied to a high-resolution quantitative magnetic resonance data set from a fixed *post mortem* multiple sclerosis brain, and validated using histology.

1 Introduction

Multiple sclerosis (MS) is classically defined as a white matter (WM) disease even though the involvement of grey matter (GM) in MS pathology has been recognized since the beginning of the 20th century. Recent immunohistochemistry (IHC) studies have shown that cortical GM lesions are common and widespread in MS brains [1, 7], yet these lesions remain extremely difficult to detect *in vivo* using MRI. The characterization and segmentation of cortical lesions *in vivo* is essential to improve our understanding of the natural course of the disease and monitor its progression.

The lack of sensitivity of MRI is due to the different pathophysiology of GM in comparison to WM lesions, in particular the absence of inflammation and edema. The contrast between cortical lesions and surrounding normal appearing grey matter (NAGM) is further dampened by the lower myelin content of GM in comparison to WM ($\sim$10%), particularly in the superficial cortical layers. The morphology of subpial lesions, that extend from the pial surface and can span several gyri, may also cause them to be concealed by partial volume effects with cerebral spinal fluid (CSF). In addition to poor local contrast, intensity driven lesion segmentation is also hindered by the presence of biological variation across healthy GM and additional variation caused by diffuse MS pathology.

The most promising MRI sequence for *in vivo* lesion detection thus far is double inversion recovery (DIR) [6], yet according to histology reports cortical

T. Jiang et al. (Eds.): MICCAI 2010, Part III, LNCS 6363, pp. 181–188, 2010.

lesions remain under-detected by this technique. Quantitative MR imaging techniques, such as relaxometry and magnetization transfer imaging, have reported abnormalities in MS patients *in vivo*; however, cortical lesions are not segmented from the NAGM in these techniques mainly due to low spatial resolution. A combined *post mortem* high resolution quantitative MRI and quantitative histology study of cortical lesions by Schmierer *et al* [9] clearly delineated cortical lesions and showed that T_1 is a predictor of neuronal density and T_2 of myelin content.

The cortical lesion segmentation technique proposed here is based on a quantitative architectural analysis method originally applied to histological data [8]. Under the assumption that the changes in myelo- and cyto-architecture laminar profiles will be reflected in the quantitative MR profiles, cortical parcellation based on laminar profile shape analysis is used to detect and delineate lesions. The methods consist of standard image processing tools adapted to analyze a unique very high-resolution 3D quantitative MRI data set of a fixed *post mortem* MS hemisphere, and validation using IHC.

2 Methods

2.1 *Post Mortem* Brain Tissue

The right hemisphere of an MS patient (79 year old female, 30 years disease duration, cause of death aspiration pneumonia) was provided by the Douglas Hospital Research Centre Brain Bank. The hemisphere was fixed in 10% buffered formalin after a *post mortem* delay of 41.25 hours, and had been fixed for approximately 4 years.

2.2 Magnetic Resonance Image Acquisition

All images were acquired on a Siemens TIM Trio 3T MRI scanner with a 32-channel receive-only head coil. The hemisphere was placed in an MR-compatible cylindrical container filled with formalin. 3D sagittal images were acquired with 0.35 mm isotropic resolution, $512 \times 512 \times 240$ matrix size and 6/8 partial Fourier phase encoding. The total acquisition time was of ∼55 hours.

Relaxometry was performed using the variable flip angle method also known as DESPOT [3]. T_1 and relative proton density, M_0, maps were calculated from two spoiled gradient echo (SPGR) images with a constant echo time (T_E) of 3.35 ms and repetition time (T_R) of 7.7 ms. The flip angles, optimized for the range of relaxation times of the fixed *post mortem* brain, were 4° and 22°. T_2 maps were derived from the measured T_1 times and two balanced steady state free precession (bSSFP) images with a fixed T_E of 3.84 ms and T_R of 7.7 ms, and optimal flip angles 20° and 70°. Each sequence was repeated 49 times, for a total scan time of ∼38.5 hours.

The magnetization transfer ratio (MTR) was calculated from two proton density weighted SPGR acquisitions with α, T_E and T_R set to 25°, 4.09 ms and 25 ms respectively. The second acquisition included the MT saturation pulse provided on the Siemens Trio 3T scanner: a 500° Gaussian pulse of $10ms$, 1200 Hz

off-resonance with a 100 Hz bandwidth. 13 repetitions were acquired for a total scan time of ∼16.5 hours.

Due to the strong variations in the RF transmission field at 3T, we acquired a B_1 map [10] to correct the nominal flip angles for both DESPOT techniques. The B_1 map was derived from two magnetization prepared turbo-spin echo (TSE) images with α, $T_{EchoSpacing}$ and T_R were set to 20°, 15 ms and 2 s respectively, with a turbo factor of 7. The acquisition was 2D with 2 mm isotropic resolution and $128 \times 128 \times 50$ matrix size. The TSE readout was preceded by an α and 2α pulse for the first and second acquisition respectively, followed by a time delay equal to half the echo-spacing.

2.3 Histology and Immunohistochemistry

Coronal slices, 1 cm thick, were cut, photographed and scanned at a lower resolution ($0.35 \times 0.35 \times 1$ mm^3) to facilitate the manual alignment of the histology to the whole hemisphere MRI. Tissue blocks representing cortical lesions and NAGM in the MR images were selected from several different cytoarchitectonic areas for paraffin embedding. Sections were cut at 5 μm, and reacted with antibodies directed against myelin basic protein (MBP), and processed in a Ventana Benchmark XT with diaminobenzidine (DAB) as chromogen. Slides were digitized using a Zeiss MIRAX Scan automated slide scanner.

2.4 Image Processing

Preprocessing. The individual raw images were linearly aligned prior to averaging [2]. The average images were used to calculate the quantitative MR maps: T_1, M_0, T_2 and MTR. The M_0 and T_2 maps were non-uniformity corrected [11] for reception field inhomogeneity and banding artifacts respectively.

The MTR map, which most resembles *in vivo* T_1-weighted contrast, was used for cortical surface extraction. The MTR image was linearly and then non-linearly aligned to the right hemisphere of the ICBM152 non-linear atlas and masked. The non-uniformity corrected MT-weighted SPGR image was used in combination with the MTR map for discrete tissue classification [14]. As shown in Figure 1, the formalin is clearly distinguishable from the surrounding GM in the sulci on the MT-weighted SPGR image due to the high contrast and resolution. The discrete tissue classification results were subsequently corrected for partial volume effects [12] and fuzzy tissue maps were created for WM, GM and formalin. Stereotaxic masks were applied to remove the brain stem and cerebellum from the tissue maps, and to label the subcortical GM and ventricles as WM. Small manual corrections of the masks were required due to the deformation caused by the fixation, otherwise the preprocessing was fully automated. An edge map of the GM/formalin interface was created by calculating the gradient of the sum of the WM and GM fuzzy tissue maps.

Cortical Boundary and Laminar Profile Extraction. The cortical boundary surfaces were extracted using FACE (Fast Accurate Cortex Extraction) [4,5],

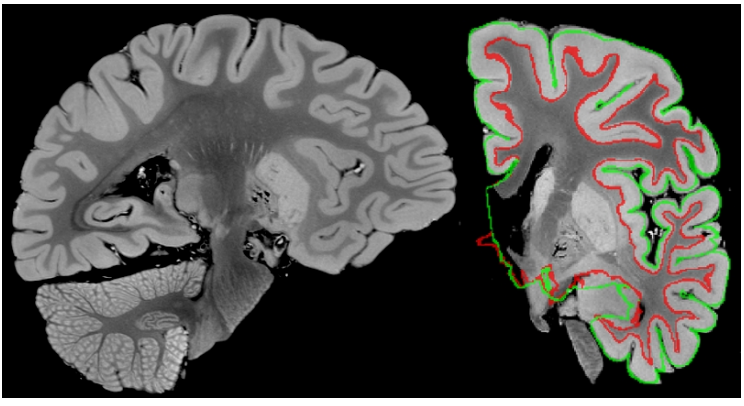

Fig. 1. Cortical surface extraction. Left: High-resolution MT-weighted SPGR image of the fixed MS hemisphere. Right: The WM and GM surfaces superimposed on the MT-weighted image in red and green respectively.

which uses deformable surfaces and a force balancing scheme. An initial surface was created by applying an iso-surface algorithm to the WM map to create a closed surface consisting of a triangulated mesh. This initial surface was then deformed iteratively to the WM/GM boundary under the influence of forces derived from the fuzzy tissue maps and gradient image. The WM surface was expanded under the influence of deformation forces derived from the surface normals, a gradient vector field, and the GM/formalin edge map. The resulting surfaces, shown superimposed on the MT-weighted image in Figure 1, consisted of approximately 240 thousand vertices uniformly distributed over the cortex.

Correspondence between vertices on the GM and WM surfaces was determined by a combination of the GM surface normals and the nearest point on the opposite WM surface. The nearest point Euclidean distances were used to constrain the results from the surface normals. The laminar profiles were extracted by sampling 20 points between corresponding vertices on the WM and GM surfaces using linear interpolation.

Laminar Profile Analysis. The laminar profile shape analysis is based on an observer-independent quantitative architecture analysis technique for cortical mapping of histological data [8]. This technique has been applied to high-resolution MRI to parcellate the visual cortex *in vivo* [13]. The first and last 10% of samples were removed to avoid contamination from neighbouring tissues. A 10-parameter feature vector was extracted from each laminar profile, including the mean amplitude and first four central moments of the profile and its absolute first derivative [8, 13]. The feature vectors derived from the 4 quantitative MR maps (T_1, M_0, T_2 and MTR) were concatenated, for a total of 40 features per profile. Each feature was z-scored to equally weigh the k-means classification. The profiles were classified into 4 clusters using a k-means classifier with a squared Euclidean distance metric. The seeds of the 4 clusters were sampled at random.

3 Results

The MBP IHC and segmentation results of a section of the superior frontal gyrus are shown in Figure 2. In the MBP section, the myelin fibers are stained brown such that the dark brown area corresponds to the densely myelinated WM and the lighter brown area corresponds to cortical GM. The light supbial band along the sulcus corresponds to a demyelinated cortical MS lesion. The corresponding laminar profile-based parcellation results differentiate the lesion, labeled white, from the neighbouring NAGM, labeled green.

The cortical segmentation results are shown on the mid-cortical surface, i.e. the median of the WM and GM surfaces, in Figure 3. The cortex was classified

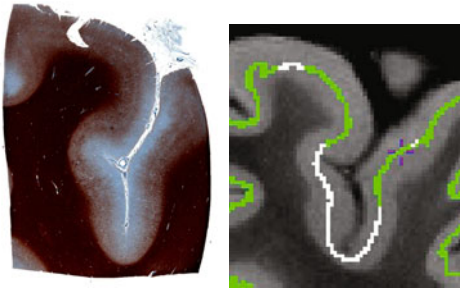

Fig. 2. Validation of cortical parcellation results with histology. Left: Tissue section of the superior frontal gyrus immuno-stained against MBP. Right: Corresponding parcellation results superimposed on an MR image. The NAGM is labeled green, and the demyelinated cortex is labeled white.

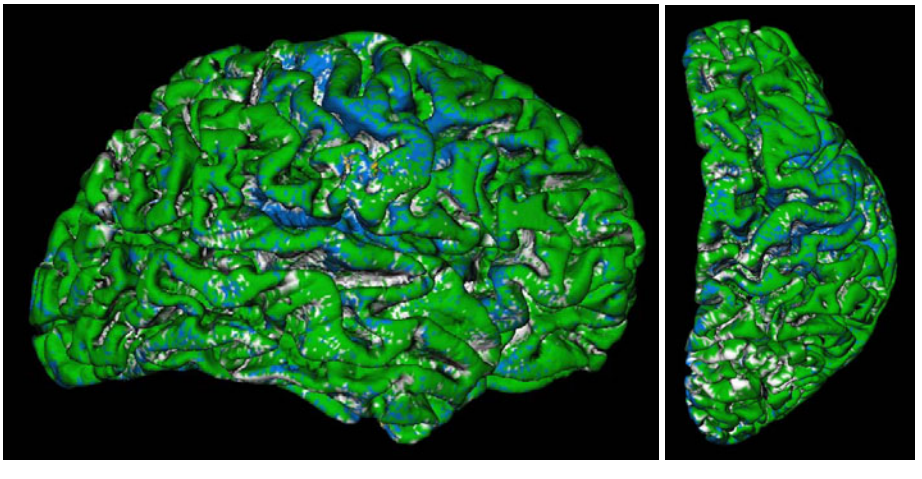

Fig. 3. Cortical parcellation results displayed on the mid-cortical surface

Table 1. Quantitative MRI results of the fixed MS hemisphere. Mean (standard deviation).

	Normal appearing GM	Cortical lesion
T_1 (ms)	187 (13)	236 (12)
T_2 (ms)	58 (6)	74 (2)
M_0	3658 (81)	3914 (69)
MTR (%)	7.35 (1.06)	7.52 (1.2)

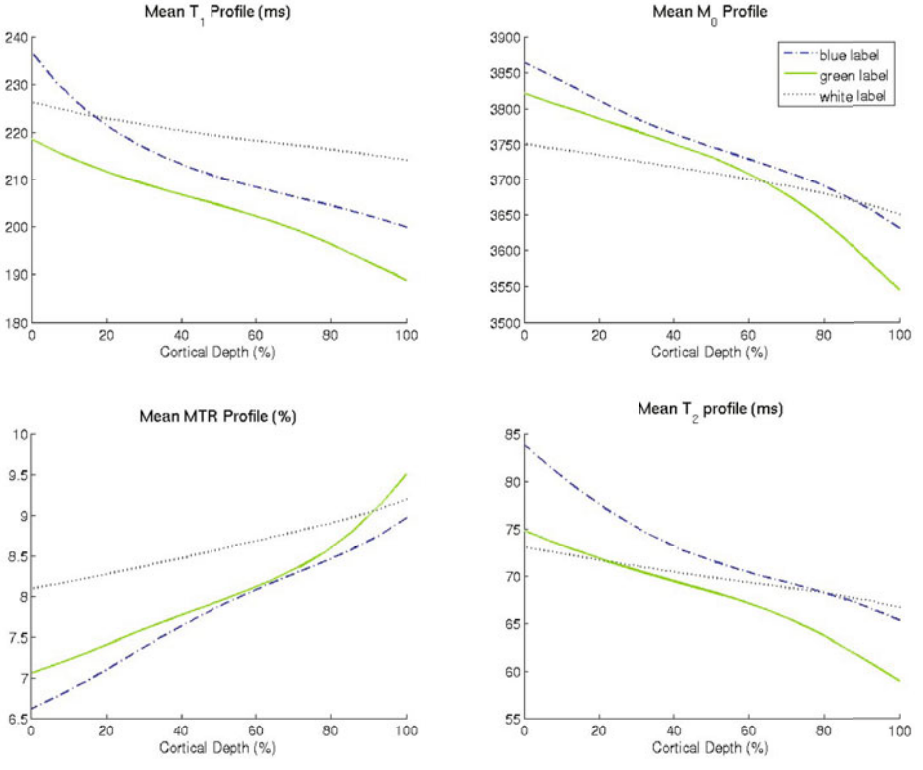

Fig. 4. Mean cortical profiles of the quantitative MR maps for each class of the cortex

into four different laminar patterns. The first class, labeled green, corresponds to NAGM. The classes labeled blue and white represent different types of cortical pathology. The fourth class represents non-cortical tissue.

Three cortical lesions were delineated in the MBP immuno-stained sections, and corresponding regions of interest (ROIs) drawn in the quantitative MRI maps. ROIs of NAGM were also chosen for comparison. Paired Student's T-tests were performed to determine the significance of the differences observed.The quantitative MRI results for the NAGM and cortical lesions are listed in Table 1. The differences in T_1, T_2, M_0 and MTR between cortical lesions and NAGM were all statistically significant ($p<0.0001$). The M_0 values were taken from the

non-uniformity corrected image. The ROIs were placed in regions that were not affected by the banding artifacts in the SSFP images. T_1 and T_2 relaxation times are higher in the cortical lesions in comparison to the NAGM. These results are in agreement with a previous fixed *post mortem* study by Schmierer *et al* [9]. The relative proton density M_0 is also increased in cortical lesions. We also observed a small but significant increase in MTR in the cortical lesions in comparison to the NAGM, whereas a decrease in MTR was reported by Schmierer *et al* in GM lesions.

The mean cortical profiles of the quantitative MR maps for each class are plotted in Figure 4, where 0% cortical depth corresponds to the GM/formalin boundary and 100% cortical depth to the WM/GM boundary. The areas labeled blue on the surfaces in Figure 3 show an increase in T_1 and T_2 times in comparison to the NAGM labeled green, in particular towards the superficial cortical layers. These regions are also characterized by an increase in M_0 and a decrease in MTR near the tissue boundaries. The areas labeled white (black dotted line in Figure 4) are characterized by a more uniform laminar profile and an increase in T_1 and MTR in comparison to the NAGM in green.

4 Discussion

We presented an automated laminar profile shape analysis technique for the segmentation of cortical MS lesions. The technique was demonstrated on a high-resolution 3D quantitative MR data set of a fixed MS hemisphere and validated with IHC. This unique combined *post mortem* quantitative MRI and IHC study is essential to improve our understanding of the relationship between MR parameters and the pathological substrates of cortical lesions.

This segmentation technique could also be applied to *in vivo* data with a lower SNR and CNR. Diffuse smoothing along the cortical mantle could be applied to improve sensitivity of profile-based morphometry to cortical lesions, in particular subpial lesions given their morphology. Furthermore, this data set can be used to guide the design of new *in vivo* acquisition techniques with optimal sensitivity to cortical pathology. We believe that this combined optimized image acquisition and analysis approach is very promising for *in vivo* lesion detection, which is essential to understand the natural course of the disease and monitor its progression.

A potential source of error in the cortical parcellation method is the inaccuracy in tissue classification and subsequent surface extraction. Cortical lesions could be misclassified as formalin/CSF, for instance, and thus remain undetected by this method.

References

1. Bo, L., Vedeler, C.A., Nyland, H.I., Trapp, B.D., Mork, S.J.: Subpial demyelination in the cerebral cortex of multiple sclerosis patients. J. Neuropathol. Exp. Neurol. 62(7), 723–732 (2003)

2. Collins, D.L., Neelin, P., Peters, T.M., Evans, A.C.: Automatic 3D intersubject registration of MR volumetric data in standardized tailarach space. Journal of Computer Assisted Tomography 18(2), 192–205 (1994)
3. Deoni, S.C., Rutt, B.K., Peters, T.M.: Rapid combined T1 and T2 mapping using gradient recalled acquisition in the steady state. Magn. Reson. Med. 49(3), 515–526 (2003)
4. Eskildsen, S.F., Ostergaard, L.R.: Active surface approach for extraction of the human cerebral cortex from MRI. In: Int. Conf. Med. Image Comput. Assist. Interv., vol. 9(Pt. 2), pp. 823–830 (2006)
5. Eskildsen, S.F., Ostergaard, L.R., Rodell, A.B., Ostergaard, L., Nielsen, J.E., Isaacs, A.M., Johannsen, P.: Cortical volumes and atrophy rates in FTD-3 CHMP2B mutation carriers and related non-carriers. NeuroImage 45(3), 713–721 (2009)
6. Geurts, J.J., Pouwels, P.J., Uitdehaag, B.M., Polman, C.H., Barkhof, F., Castelijns, J.A.: Intracortical lesions in multiple sclerosis: improved detection with 3D double inversion-recovery MR imaging. Radiology 236(1), 254–260 (2005)
7. Kutzelnigg, A., Lucchinetti, C.F., Stadelmann, C., Bruck, W., Rauschka, H., Bergmann, M., Schmidbauer, M., Parisi, J.E., Lassmann, H.: Cortical demyelination and diffuse white matter injury in multiple sclerosis. Brain 128(Pt. 11), 2705–2712 (2005)
8. Schleicher, A., Morosan, P., Amunts, K., Zilles, K.: Quantitative architectural analysis: A new approach to cortical mapping. J. Autism Dev. Disord. (2009)
9. Schmierer, K., Parkes, H.G., So, P.W., An, S.F., Brandner, S., Ordidge, R.J., Yousry, T.A., Miller, D.H.: High field (9.4 Tesla) magnetic resonance imaging of cortical grey matter lesions in multiple sclerosis. Brain 133(Pt. 3), 858–867 (2010)
10. Sled, J.G., Pike, G.B.: Correction for B1 and B0 variations in quantitative T2 measurements using MRI. Magn. Reson. Med. 43(4), 593 (2000)
11. Sled, J.G., Zijdenbos, A.P., Evans, A.C.: A nonparametric method for automatic correction of intensity nonuniformity in MRI data. IEEE Trans. Med. Imaging 17(1), 87–97 (1998)
12. Tohka, J., Zijdenbos, A., Evans, A.: Fast and robust parameter estimation for statistical partial volume models in brain MRI. NeuroImage 23(1), 84–97 (2004)
13. Walters, N.B., Eickhoff, S.B., Schleicher, A., Zilles, K., Amunts, K., Egan, G.F., Watson, J.D.: Observer-independent analysis of high-resolution MR images of the human cerebral cortex: In vivo delineation of cortical areas. Hum. Brain Mapp. 28(1), 1–8 (2007)
14. Zijdenbos, A.P., Forghani, R., Evans, A.C.: Automatic 'pipeline' analysis of 3D MRI data for clinical trials: application to multiple sclerosis. IEEE Transactions on Medical Imaging 21(10), 1280–1291 (2002)